

Raman study of anharmonic effects in $\text{Pr}_{0.5}\text{Ca}_{0.5}\text{MnO}_3$ thin filmsA. Tati,¹ E. L. Papadopoulou,¹ D. Lampakis,¹ E. Liarokapis,¹ W. Prellier,² and B. Mercey²¹*Department of Physics, National Technical University of Athens, GR-15780 Athens, Greece*²*Laboratoire CRISMAT, CNRS UMR 6508, Bd Marechal Juin, F-14050 Caen Cedex, France*

(Received 30 August 2002; revised manuscript received 31 January 2003; published 31 July 2003)

We report low-temperature and hydrostatic pressure Raman measurements in $\text{Pr}_{0.5}\text{Ca}_{0.5}\text{MnO}_3$ thin films grown on SrTiO_3 and LaAlO_3 substrates. From the low-temperature dependence of the modes related with the Jahn-Teller distortions of the octahedra, it is found that an increase appears in their relative intensities at temperatures close to the charge-ordering phase transition. Two rotational modes of vibration of the octahedra show an anharmonic behavior. Strains from the substrate do not induce any shift or new modes in the Raman spectra probably due to their relaxation from the interface towards the surface of the films. From the different orientation of the two films, the symmetry of certain modes has been identified.

DOI: 10.1103/PhysRevB.68.024432

PACS number(s): 75.47.Gk, 78.30.-j, 63.20.-e

I. INTRODUCTION

In the past decade, there has been an increased interest in doped manganites exhibiting colossal magnetoresistance (CMR).¹ These materials of type $\text{R}_{1-x}\text{A}_x\text{MnO}_3$ consist of a trivalent rare earth R (e.g., La, Pr, Nd, . . .) replaced by a divalent alkaline earth A (e.g., Ca, Sr, . . .). One of the most exciting phenomena of these materials is the charge ordering (CO). This phenomenon is observed when the electrons become localized in real space and the heterovalent cations in the two sublattices (Mn^{+3} and Mn^{+4}) become ordered.

The system $\text{Pr}_x\text{Ca}_{1-x}\text{MnO}_3$ is a compound with a rich phase diagram and a more distorted structure than other CMR materials. Polycrystalline samples and single crystals of this compound have been studied, for different x , with various methods such as x -ray synchrotron and neutron diffraction,² Raman scattering,^{3,4} and resistivity.⁵ It has been shown that at zero applied magnetic field, the material is a paramagnetic insulator and no transition to a metallic state takes place. The application of a strong magnetic field can induce an insulator to metal transition.⁵ Charge ordering in $\text{Pr}_x\text{Ca}_{1-x}\text{MnO}_3$ occurs in the regime $0.3 \leq x \leq 0.75$ at the temperature range 220–240 K, depending on the amount of Ca doping. Within this CO phase, there is a magnetic transition to an antiferromagnetic insulating phase at temperature $T_N < T_{CO}$, which for our compound ($x=0.5$) is at ~ 180 K. For lower Ca concentrations ($0.3 \leq x \leq 0.4$), another transition has been observed to a spin-canted insulating phase at a temperature $T_{CA} < T_N$. T_{CA} decreases with Ca concentration and reaches a value below 50 K for $x=0.4$.⁶ This however, has been argued by Cox *et al.*,² who found that the exposure of a $\text{Pr}_{0.7}\text{Ca}_{0.3}\text{MnO}_3$ sample to an x -ray beam at low-temperature discloses a phase-segregation phenomenon, where the CO insulating phase coexists with a charge delocalized (CD) metalliclike phase. The charge-ordering phenomenon seems to be optimized for $x=0.5$, where the carriers are exactly commensurate with the 1:1 ordering of the $\text{Mn}^{+3}:\text{Mn}^{+4}$ species.⁵ Across the CO transition, where the carriers become strongly localized, strong electron-phonon interactions induce structural changes in the material. Fur-

thermore, a lowering of the symmetry takes place and a change of 0.6–2.4% in the lattice parameters has been observed.^{3,5} However, these structural transitions that accompany the CO are not observed in the thin films.⁷

It has been shown for bulk samples that a slight variation of the Mn-O bond length or the Mn-O-Mn angle modifies the physical properties of the material.⁸ In the case of thin films, these variations of the bond length or the bond angle may be due to the strains that the substrate imposes on the thin film. These lead to changes in the properties, comparing to the bulk material. For example, it was found that the critical magnetic field required to destroy CO is strongly reduced when the compound is made in the form of a thin film.⁷ Another parameter that may affect the physical properties of the films is the orientation of the growth of the film on the substrate. Since most of the technological applications require thin films, it is of great importance to understand their physical properties.⁷

An extensive amount of Raman data exist for various compounds of the $\text{R}_{1-x}\text{A}_x\text{MnO}_3$ series and an assignment for most of the phonons that appear has been proposed.^{9,10} To the best of our knowledge, for the specific compound, the Raman data exist only for the $x \approx 0.35$ (Ref. 3) and $x \approx 0.37$ (Ref. 4) members of the $\text{Pr}_{1-x}\text{Ca}_x\text{MnO}_3$ series. The latter has shown an anomalous temperature dependence for two of the A_g symmetry phonons, which was attributed to the spin-phonon coupling.⁴ In this work we have investigated the temperature dependences of the Raman active phonons in the range 78–295 K of two $\text{Pr}_{1-x}\text{Ca}_x\text{MnO}_3$ thin films deposited on two different substrates that induce tensile and compressive strains on the film. The compound was doped with $x=0.5$, for optimum CO. A detailed analysis of the Raman spectra through the CO transition has been carried out in order to investigate the phonon modifications related with this transition. Furthermore, an analysis of the temperature and hydrostatic pressure dependence of the strong Raman active phonons has been performed revealing a considerable anharmonicity for two rotation modes of the Mn-O octahedra. Based on the Raman scattering selection rules from the two films of different orientation, an assignment

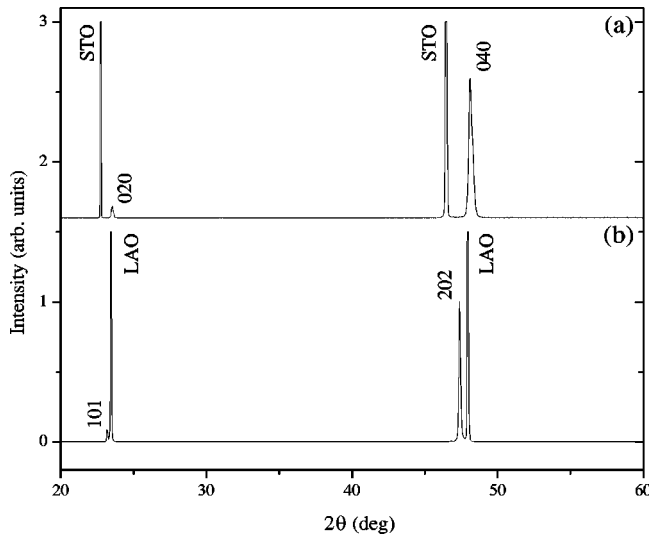


FIG. 1. The XRD results obtained at room temperature for the film deposited on the two substrates SrTiO₃ (a) and LaAlO₃ (b).

for certain modes has been induced. Finally, the effects of the strains from the two substrates on the Raman spectra of the films are discussed.

II. EXPERIMENT

Films of Pr_{0.5}Ca_{0.5}MnO₃ (PCMO) of thickness 180 nm were grown *in situ* using the Pulsed Laser Deposition technique deposited on two different substrates with the [100] orientation, a SrTiO₃ (STO), which is cubic with a lattice constant $a=3.905$ Å, and a LaAlO₃ (LAO), which is pseudocubic with $a=3.789$ Å. The substrates were kept at a constant temperature of 725°C during the deposition, which was carried out at a pressure of 300 mTorr of flowing oxygen. After the deposition, the samples were slowly cooled to room temperature (RT) at a pressure of 500 Torr of O₂. A detailed optimization of the growth procedure was completed and described previously.^{11,12} The structural study was carried out by *x*-ray diffraction (XRD) using a Seifert XRD 3000P for the $\Theta-2\Theta$ scans (Cu $K\alpha$, $\lambda=1.5406$). The films were shown to be homogeneous and the structure corresponds exactly to the composition of the target (i.e., Pr_{0.5}Ca_{0.5}MnO₃) in the limit of accuracy.

The structure of the bulk Pr_{0.5}Ca_{0.5}MnO₃ was found to be orthorhombic ($Pnma$) with lattice constants $a=5.395$ Å, $b=7.612$ Å, and $c=5.403$ Å.¹³ Figures 1(a) and 1(b) show a typical $\Theta-2\Theta$ scan recorded for a film of PCMO/STO and PCMO/LAO, respectively. The films were of a single phase and highly crystallized, as seen from the sharp and intense diffraction peaks. It has been found that the films were [010] oriented (i.e., with the [010] axis perpendicular to the substrate plane) on the STO substrate and [101] oriented on the LAO substrate. This orientation was the result of the lattice mismatch between the film and the substrate.¹⁴ Using the XRD results, the out-of-plane lattice parameter of the substrates was calculated to be 3.778 Å for STO and 3.834 Å for LAO, confirming that the film is under tensile stress on STO and under compression on LAO.

The Raman spectra were obtained using a T64000 Jobin Yvon triple spectrometer, equipped with a liquid nitrogen cooled charge coupled device and a microscope. The 530.9 nm and 647.1 nm lines of a Kr⁺ laser and the 457.9 nm, 488 nm, 514.5 nm lines of an Ar⁺ laser were used for excitation, at low power, which was kept fixed during the measurements at the level of ~ 0.1 mW on the surface of the film. Raman spectra of the film were measured at a temperature region from 78 K to 295 K. A backscattering geometry was used, with the sample placed under the microscope with $a\times 100$ magnification lens. For the low-temperature measurements, an Oxford cryostat was used, appropriately modified for the application of the scattering selection rules. The temperature instability was less than 1 K and the local heating due to the laser beam was estimated to be less than 10 K.^{15,16} All the spectra have been corrected for the Bose thermal factor at the nominal temperatures, but any uncertainties from a laser local heating could not induce appreciable changes in the shapes of the peaks. Hydrostatic pressure measurements were also carried out at RT using a Merrill-Bassett-type diamond anvil cell, operated in the backscattering geometry. The transmitting medium was a 4:1 methanol:ethanol mixture and the pressure was calculated by inserting a silicon single crystal inside the gasket. The accumulation times of the spectra were of the order of 5–6 h at ambient conditions and at low-temperatures. For the high-pressure measurements, the accumulation times were of the order of 10 h. The spectrometer was calibrated just before and right after each measurement, using a silicon wafer as a reference.

III. RESULTS

In Fig. 2 typical Raman spectra of the PCMO/STO film excited by the 647.1 nm laser line are shown for the temperature range 78–295 K. The most pronounced peaks displayed for the entire temperature range are centered (at 78 K) around 85 cm⁻¹, 268 cm⁻¹, 300 cm⁻¹, 476 cm⁻¹, and 605 cm⁻¹. In addition, there is a broad feature at ~ 133 cm⁻¹ (at 78 K), which at RT appears as a wide peak of energy at ~ 143 cm⁻¹. At low-temperatures additional peaks emerge at 230, 530, and 640 cm⁻¹, which cannot be distinguished at RT. The Raman spectra obtained from polycrystalline samples of Pr_{0.65}Sr_{0.35}MnO₃ are similar but contain at RT fewer peaks at similar energies, i.e., ~ 80 cm⁻¹, 145 cm⁻¹, 475 cm⁻¹, and 610 cm⁻¹, while at lowering the temperature the peak at 230 cm⁻¹ is also present.³ In Figs. 3 and 4, the spectra obtained by the 530.9 nm and 488 nm laser excitation lines, respectively, are shown. New modes seem to appear at 430, 460, and 660 cm⁻¹. It is seen that the excitation photon energy does not modify the energy of the phonon modes that appear, while the relative intensity of the wide band around ~ 476 cm⁻¹ increases with the 647.1 nm excitation wavelength. This agrees with Abrashev *et al.*,¹⁷ who have found that the relative intensity of the strong peaks, which in the LaMnO₃ compound appear at 516 cm⁻¹ and 640 cm⁻¹, increases with decreasing excitation photon energy, in accordance with theoretical calculations.^{17,18} In the system LaSr₂Mn₂O₇, Argyriou *et al.*¹⁹ have observed a resonance with the 514.5 nm laser line as the corresponding to the 476 cm⁻¹ mode was increasing in intensity for all tem-

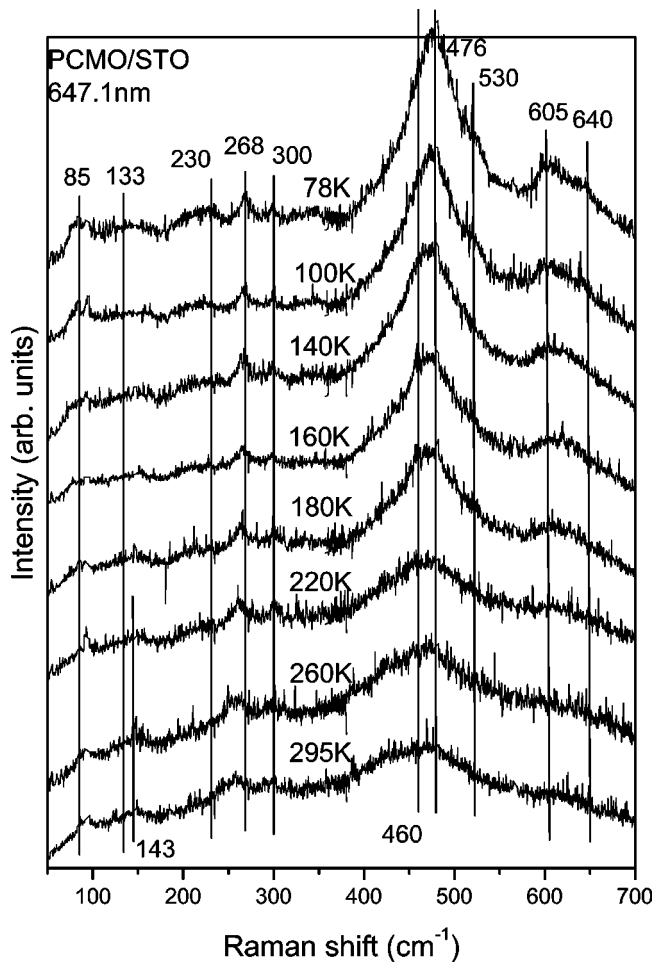


FIG. 2. Typical Raman spectra from the PCMO/STO film with the 647.1 nm excitation wavelength in the temperature range 78–295 K. The spectra have been corrected with the Bose thermal factor.

peratures studied. No variation in intensity has been observed in our system in this mode with the 514.5, 488 (Figs. 3 and 4), and the 457.9 nm laser lines. Only with the 514.5 nm wavelength, the two modes at 460 cm^{-1} and 476 cm^{-1} could be clearly discriminated as the corresponding modes of Ref. 19. In addition, we have not observed new modes or spectral modifications with the 488 nm excitation wavelength (Fig. 4) and we believe that the completely different spectrum found by Dediu *et al.*³ might be due to an impurity phase. The spectra reported here are typical for all disordered manganites. The crystal structure of $\text{Pr}_{1-x}\text{Ca}_x\text{MnO}_3$ is the same as that of LaMnO_3 . It is therefore possible to follow for the modes of $\text{Pr}_{1-x}\text{Ca}_x\text{MnO}_3$ the symmetry assignment used by Iliev *et al.* for LaMnO_3 .⁹

Both low-energy bands at 85 cm^{-1} and 133 cm^{-1} show an unusual increase in energy with increasing temperature. As seen in Fig. 2, at low-temperatures, the first mode clearly consists of two much narrower bands. Something similar happens for the very broad structure at 133 cm^{-1} , which must be an independent mode from the one at 143 cm^{-1} observed at RT and seems to consist of several peaks, with the most pronounced ones at those two energies. According

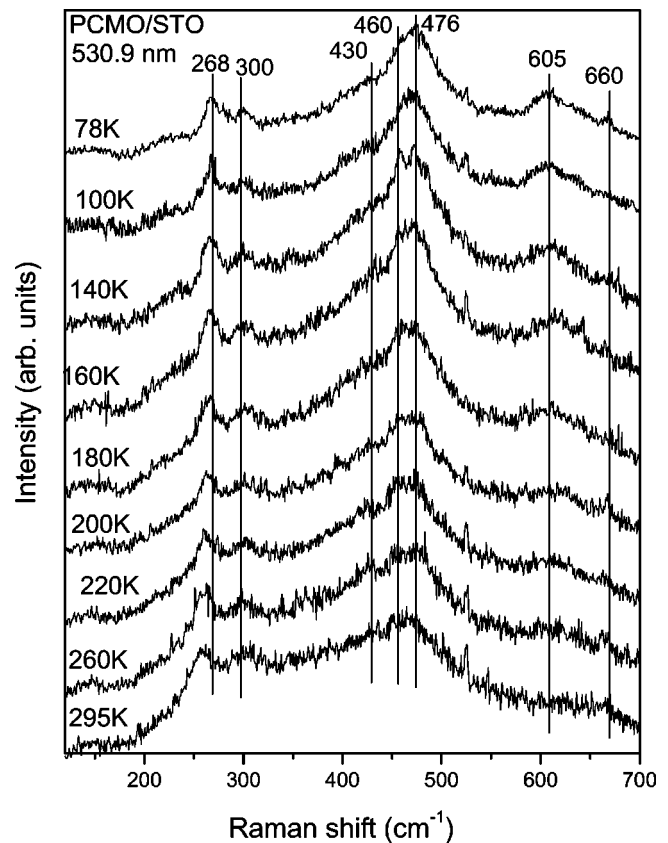


FIG. 3. Typical Raman spectra from the PCMO/STO film with the 530.9 nm excitation wavelength in the temperature range 78–295 K. The spectra have been corrected with the Bose thermal factor.

to Iliev *et al.*,⁹ the modes at 85 and 133 cm^{-1} are of A_g symmetry and they are very weak at all excitation wavelengths. These low-energy modes are more easily observed with the 647.1 nm excitation line. It is possible that the apparent softening of these modes with decreasing temperature is the result of modifications in the relative intensities of the various lines that constitute each band.

On the contrary, the mode centered around $\sim 268 \text{ cm}^{-1}$ (at 78K) observed only in parallel polarizations, as shown in Fig. 5, which shows the strong modes for various scattering polarizations, is very well defined. In Fig. 6(a), the phonon energy is plotted for different temperatures. It shows a strong dependence on temperature, decreasing in energy by 12 cm^{-1} in the range 78–300 K. At $T \approx 225$ K, there is a more rapid softening of this mode. This temperature is in the range of the expected T_{CO} . A similar temperature dependence is seen in Fig. 6(b), for the energy of the other strong but wide band around 476 cm^{-1} , which changes slightly at T_{CO} . The width of both bands is also affected appreciably by the variation of the temperature.

In Figs. 2–4 it is seen that the peak at 300 cm^{-1} has a different behavior, being temperature independent. This neighbor mode to the 268 cm^{-1} could correspond to a phonon of B_{2g} symmetry with energy at $\sim 308 \text{ cm}^{-1}$ or a tilting mode of A_g symmetry at 284 cm^{-1} (in LaMnO_3).⁹ As shown in Fig. 5, it only appears in parallel polarizations and

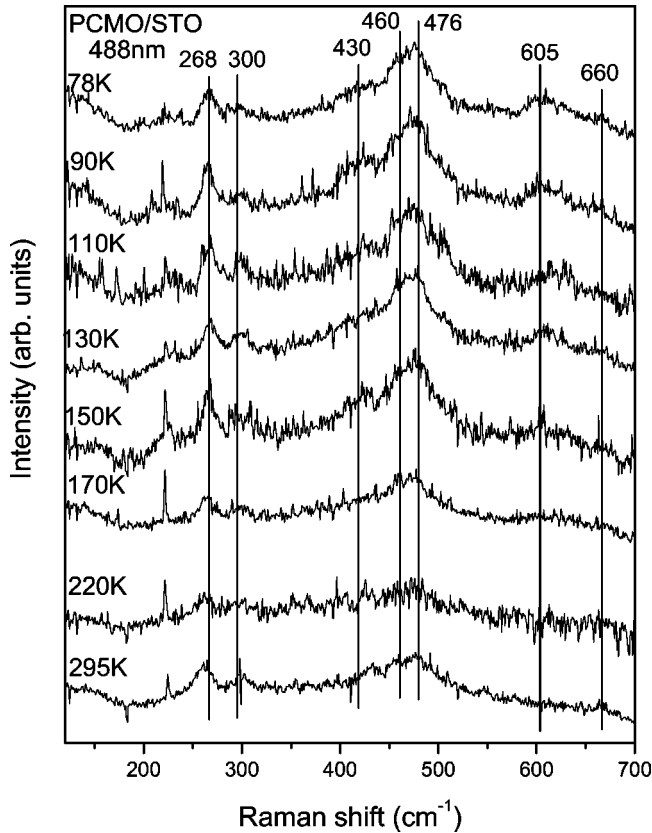


FIG. 4. Typical Raman spectra from the PCMO/STO film with the 488 nm excitation wavelength in the temperature range 78–295 K. The spectra have been corrected with the Bose thermal factor.

its relative energy to the 268 cm^{-1} mode coincides with the ratio of the corresponding A_g modes of $\text{La}_{1-x}\text{Mn}_x\text{O}_3$,^{9,20} we attribute it to the tilting vibrations of the octahedra.⁹ However, contrary to the case of the mode at $\sim 268\text{ cm}^{-1}$, its energy and width does not seem to be modified with temperature.

At lowering the temperature below 140 K, a new wide band at $\sim 230\text{ cm}^{-1}$ becomes visible, which must be identified as the one that has sometimes been observed at the same energy and low temperatures by other authors.^{3,17} This mode has been identified as a soft mode, by these authors, and has been assigned to a rotational-like mode. However, we did not observe the softening of this mode, but only its disappearance with increasing temperature.

The two phonons centered at 476 cm^{-1} and 605 cm^{-1} are related to Jahn-Teller distortions of the octahedra. As seen in Fig. 2, their relative intensities to the lower-energy modes increase considerably at lowering the temperature from RT to 78 K. This has also been observed for the other two excitation wavelengths, but the increase in intensity is not so strong. The peak at 476 cm^{-1} , which has previously been attributed to the asymmetric stretching of A_g symmetry,^{9,10} becomes sharper and moves slightly to higher energies with decreasing temperature. Our measurements show that this mode has the B_{2g} symmetry (Fig. 5). The other peak at 605 cm^{-1} is more pronounced at lower temperatures and is assigned to the symmetric stretching of the

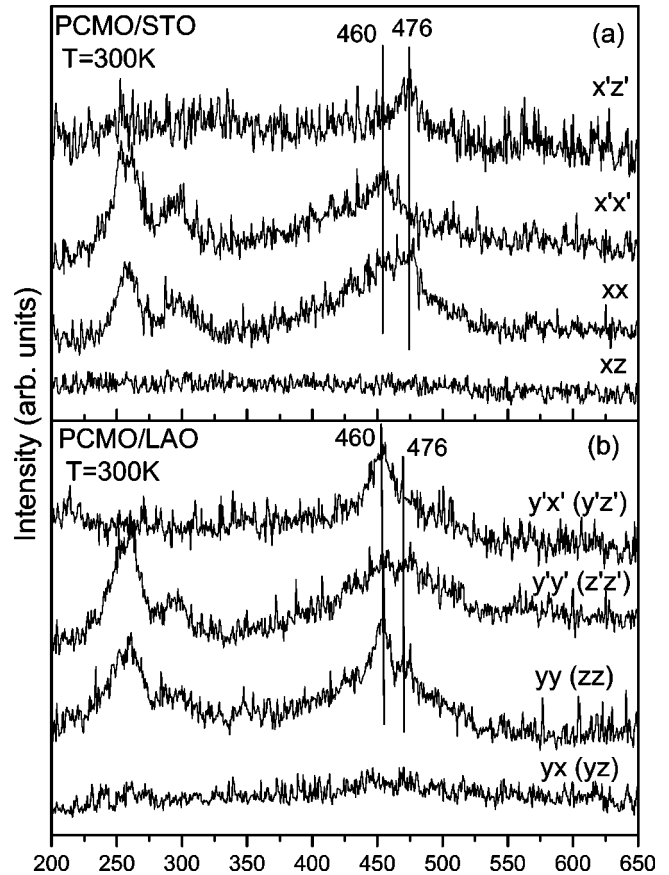


FIG. 5. Polarized Raman spectra measured on the PCMO/STO (a) and the PCMO/LAO (b) films using the 514.5 nm laser line. The scattering configuration for each spectrum is indicated, where the first symbol indicates the direction of the polarization of the incident light and the second the polarization of the scattered light. In the case of the PCMO/LAO film, there is a mixture of polarizations as indicated by the parentheses.

basal oxygens of the octahedra (B_{1g} symmetry).¹⁰ According to Iliev *et al.* though,⁹ this mode is of B_{2g} symmetry. Due to the weakness of the mode, we could not make a more definite assignment. Below $\sim 220\text{ K}$, the two bands at 476 cm^{-1} and 605 cm^{-1} contain numerous peaks that overlap one another. This behavior has been attributed to the formation of the CO state.³ As shown in Figs. 2–4, at low-temperatures, the mode at 605 cm^{-1} is accompanied by at least two more bands centered around $\sim 640\text{ cm}^{-1}$ and 660 cm^{-1} . Moreover, the mode at 476 cm^{-1} is accompanied by a peak at slightly lower energy ($\sim 460\text{ cm}^{-1}$) and two other weaker bands centered at $\sim 430\text{ cm}^{-1}$ and $\sim 530\text{ cm}^{-1}$. Our selection rules on the LAO sample with the [101] film orientation have shown that the 460-cm^{-1} mode has the B_{1g} or the B_{3g} symmetry (Fig. 5). Our data also indicate that the mode at $\sim 430\text{ cm}^{-1}$ has the B_{2g} symmetry. At low-temperatures, the spectra show pronounced modifications, especially in the temperature range 140–160 K, where the 476 cm^{-1} wide band appears as a double peak for the excitation with the 530.9 nm laser line (Fig. 3). A similar double structure has been observed in the $\text{LaSr}_2\text{Mn}_2\text{O}_7$ perovskite with the 514.5 nm excitation line and it was attributed to a resonance

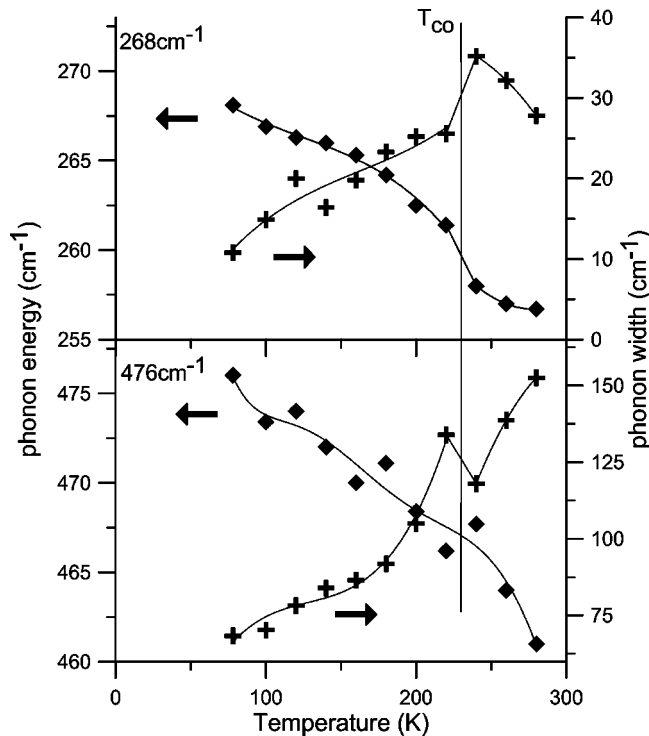


FIG. 6. The temperature dependence of the energy (squares) and width (crosses) of the strong modes at 268 cm^{-1} and 476 cm^{-1} wide bands. The continuous lines are guides to the eye.

effect driven by the formation of a CO state.¹⁹ This double structure is less pronounced at higher temperatures or the other excitation wavelengths and it is induced from the spectra only by the abnormal broadening of the main mode at $\sim 476\text{ cm}^{-1}$. At 260 K even this broadening begins to disappear and at 295 K cannot be seen. According to Ref. 5, the bulk compound should pass to a charge-ordered state at a temperature $\sim 240\text{ K}$, while in the PCMO/STO film the transition temperature is slightly lower, at 225 K.¹¹ This is the temperature where the widening of the 476 cm^{-1} mode and the increase of the intensity of the bands at 476 cm^{-1} and 605 cm^{-1} appears.

In Fig. 7, one additional very weak mode is observed in the PCMO/LAO film with energy at $\sim 560\text{ cm}^{-1}$. With increasing temperature, the intensity of this weak mode decreases rapidly and cannot be observed at room temperature. On the contrary, the low-energy mode at $\sim 143\text{ cm}^{-1}$ remains strong and does not shift with energy at all temperatures. In the PCMO/STO film, the similar mode appears weaker at temperatures close to RT while at 78 K only the mode at 133 cm^{-1} appears (Fig. 2). It seems that the 143 cm^{-1} wide band has a different polarization selection rule than the 133 cm^{-1} phonon observed in the PCMO/STO film. This could explain its appearance in the LAO substrate, where the film has been developed at a different orientation.

IV. DISCUSSION

One question to be answered is the effect of the strain from the substrate to the physical properties of the films. The

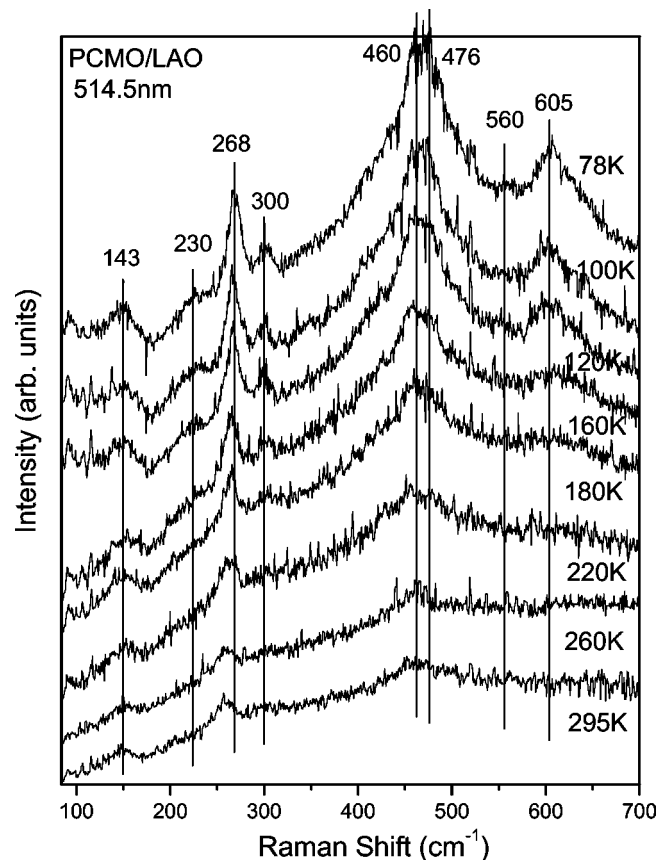


FIG. 7. Typical Raman spectra for selected low-temperatures measured on the PCMO/LAO film using the 514.5 nm laser line. All spectra have been corrected with the Bose thermal factor.

splitting of the high-energy modes could be possibly associated with the presence of strains from the substrate. The total strain in the films should be the original strain introduced during preparation from the lattice mismatch, plus any thermally induced from the differences in the thermal expansion coefficient between the film and the substrate. The latter should vary with temperature, and therefore the splitting of the modes should show a linear dependence with temperature. Within the detection limit ($<1\text{ cm}^{-1}$) no shift has been observed in the splitting of the high-energy modes. This implies that the additional modes that appear in the Raman spectra at low-temperatures are not related to any strain effects.

The XRD measurements of the lattice constants of the substrates of the two films have shown that they are under 1.2% tensile (LAO) and 3.3% compressive (STO) strains. The presence of such strains implies that the corresponding films are also strained. Our hydrostatic pressure measurements (Fig. 8) have shown that the band at 476 cm^{-1} shifts roughly with a rate $6\text{ cm}^{-1}/\text{GPa}$, while the mode at 268 cm^{-1} at almost half this rate. We do not know the bulk modulus to calculate the phonon shift that corresponds to the strain of the films, but an approximate value of $\sim 150\text{ GPa}$ from $\text{La}_{0.83}\text{Sr}_{0.17}\text{MnO}_3$ can be used for an estimate.²¹ One then expects that even a strain of the order of 1% could induce considerable shifts of $\sim 10\text{ cm}^{-1}$ and $\sim 4\text{ cm}^{-1}$ in

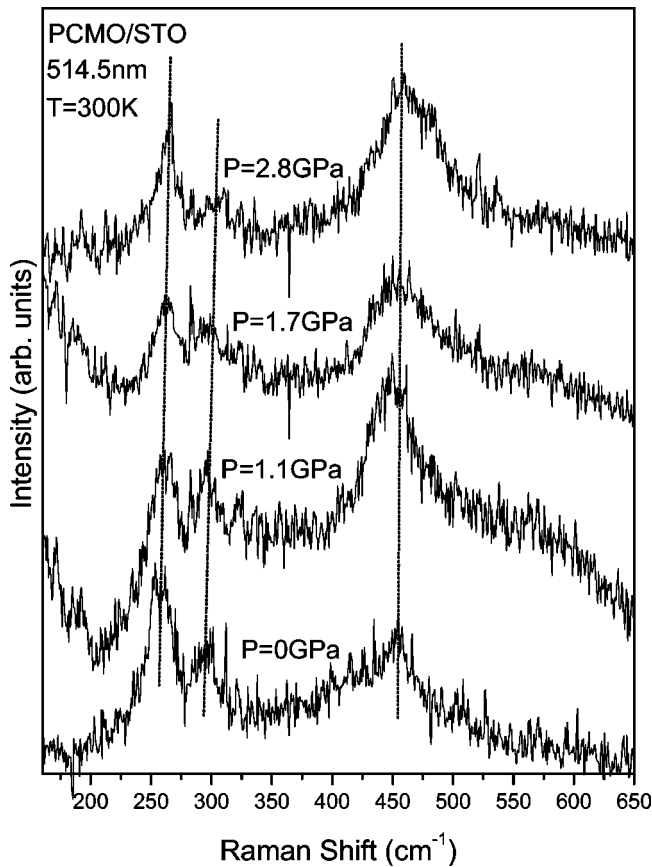


FIG. 8. Typical Raman spectra for selected different hydrostatic pressures measured on the PCMO/STO film using the 514.5 nm laser line. The dashed lines indicate the shift of the average peak position of the three bands.

the energy of the above two phonons. Comparing Figs. 3 and 7 it is seen that the 476 cm^{-1} mode appears in the LAO substrate with the same energy as in the STO, independent of the built in compressive or tensile strains. As the Raman scattering probes mainly the surface, it is possible that the strains are relaxed at the surface of the films (180 nm) used in this study. On the other hand, resistivity measurements, which are bulk measurements, may have detected the strains developed at the interface.¹¹

One should remark that differences are observed between the relative intensities of the high-energy phonons in the films from the two substrates. In the PCMO/STO film, the 476 cm^{-1} phonon is stronger than the mode at 460 cm^{-1} (Figs. 2–4). However, in the PCMO/LAO film, the situation is reversed, with the 460 cm^{-1} mode slightly stronger than the 476 cm^{-1} one (Fig. 7). In addition, in Fig. 5, the Raman spectra of the two samples are shown for different scattering configurations (xx , xz , $x'x'$ and $x'z'$). In the $x'z'$ spectrum of PCMO/STO, the 476 cm^{-1} mode appears whereas the 460 cm^{-1} mode is absent. In the PCMO/LAO film, the reversed situation is realized. This leads to the conclusion that the 476 cm^{-1} mode has B_{2g} -like symmetry and the 460 cm^{-1} the B_{1g} or the B_{3g} symmetry. Abrashev *et al.*,²⁶ however, in films of $\text{CaMnO}_3/\text{LAO}$ and $\text{CaMnO}_3/\text{STO}$, have assigned the lower-energy mode, of the two corre-

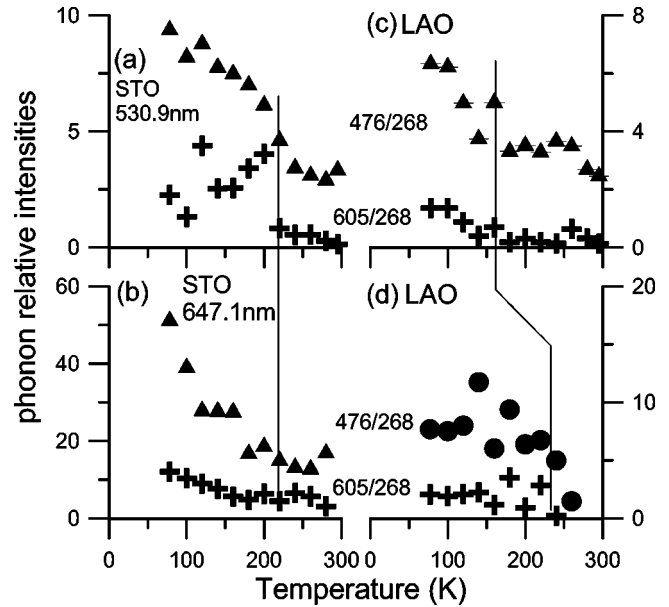


FIG. 9. The temperature dependence of the relative intensity of the high-energy wide bands at $\sim 476 \text{ cm}^{-1}$ (Δ) and $\sim 605 \text{ cm}^{-1}$ ($+$) to the phonon at $\sim 268 \text{ cm}^{-1}$ for both substrates. (a),(b) The PCMO/STO film probed with the 530.9-nm and the 647.1 nm laser lines. (c) and (d) The PCMO/LAO film probed with the 514.5 nm laser line. In (a), (b), and (d), the measurements were done with increasing temperature, while in (c) the temperature was varied up and down, and the hysteresis is clearly shown.

sponding phonons, to B_{2g} and the higher energy one to A_g . However, the $\text{CaMnO}_3/\text{LAO}$ and $\text{CaMnO}_3/\text{STO}$ films were $[100]$ oriented. In our case, the PCMO/LAO film is $[101]$, whereas the PCMO/STO is $[010]$ oriented. This different orientation of the films has made possible to differentiate the B_{1g} (or B_{3g}) symmetry of the lower-energy mode, from the B_{2g} symmetry, which in our case was the higher-energy mode (Fig. 5). Furthermore, the relative intensity of the 605 cm^{-1} phonon to the one at $\sim 640 \text{ cm}^{-1}$ has a similar behavior with the 476 cm^{-1} mode to the 460 cm^{-1} one. While the phonon at $\sim 640 \text{ cm}^{-1}$ can be distinguished (mainly at low temperatures) in the PCMO/STO film (Figs. 2 and 3), the situation changes in the PCMO/LAO compound, where the 605 cm^{-1} mode completely dominates whereas the 640 cm^{-1} and 660 cm^{-1} bands can be hardly seen (Fig. 7). We believe that these spectral modifications are mainly due to the different orientation of the two films, and the lattice mismatch.²⁶

Figures 9(a) and 9(b) present the modifications induced by temperature to the relative intensity of the two high-energy bands at 476 cm^{-1} and 605 cm^{-1} , when compared to the low-energy phonon at 268 cm^{-1} . It is clear that for the PCMO/STO film, there is an increase in the relative intensities of these modes for the 647.1 nm and 530.9 nm excitation wavelengths, below $\sim 220 \text{ K}$. A similar behavior has been observed with the 488 nm laser line. Due to the transition to a charge-ordered phase with more localized carriers, the intensity of all modes is expected to increase in this phase. The preferential increase of the intensity of the high-energy bands would imply that their screening from the carriers is much

stronger than for the mode at 268 cm^{-1} . This must be related with the association of these modes with the Jahn-Teller distortions. In the PCMO/STO film, the CO phase appears at $\sim 225 \text{ K}$,¹¹ which is in good agreement with our Raman data. One can also see that the increase in the relative intensity of the modes is five times larger for the excitation with the 647.1 nm wavelength. It is unclear whether this considerable increase is affected also by the strains as the red light probes deeper inside the film and closer to the interface with the substrate.

In the PCMO/LAO film, the Raman data indicate that the change in intensity occurs at different temperatures $\sim 170 \text{ K}$ [Fig. 9(c)] or $\sim 235 \text{ K}$ [Fig. 9(d)]. The first value has been obtained on lowering the temperature, contrary to the case of (a), (b), and (d) where the temperature, once it had reached the lowest value (78 K), was gradually increased until it reached RT. This difference is due to the hysteresis effect, which is very characteristic in these compounds.¹¹ In Fig. 9(d) the value for the intensity variation obtained for the LAO film, but with increasing temperature, agrees, within error, with the corresponding value for the PCMO/STO film. This is another indication that strains are not affecting the surface of the films, which we probe with the Raman scattering. Furthermore, the value of the temperature where the spectral changes occur, points out the formation of the charged-ordered phase, bringing more information about these compounds from the Raman measurements.

The reduction of a phonon energy with increasing temperature is partially due to the volume effect, i.e., the expansion of the unit cell with heating, and partially to a pure anharmonic effect (if the volume was kept fixed). Since the 268 cm^{-1} , 300 cm^{-1} , and 476 cm^{-1} bands were measured under hydrostatic pressures, an estimate of the pure anharmonicity can be obtained provided that the thermal expansion coefficient and the elastic constants of the compound are known. Up to now, there are no measurements of the thermal expansion coefficient for the compound in bulk sample or films. However, one can get a rough estimate using the linear thermal expansion of a similar CMR compound. The $\text{La}_{0.83}\text{Sr}_{0.17}\text{MnO}_3$ compound was found to be isotropic with a volume thermal expansion coefficient $\beta_v = 30 \times 10^{-6}$.²² A very similar value at RT has been found from studies of the charge-ordered polycrystalline compounds $\text{Pr}_{0.75}\text{Sr}_{0.25}\text{MnO}_3$ (Ref. 23) and $\text{La}_{0.67}\text{Ca}_{0.33}\text{MnO}_3$,²⁴ it is therefore possible to use this value.

From the chain differentiation rule, one can prove²⁵ that in the case of an isotropic approximation, the temperature dependence of the phonon energy is written as

$$\left(\frac{d\omega}{dT}\right)_P = -\frac{\beta_v}{k_v} \left(\frac{\partial\omega}{\partial P}\right)_T + \left(\frac{\partial\omega}{\partial T}\right)_V, \quad (1)$$

where the first term on the right-hand side of the equation stands for the implicit (volume-driven) effect and the second for the explicit (amplitude-driven) effect. In the case of a nonisotropic (tetragonal) crystal, one needs to add a correction α to the above equation,²⁵

$$\alpha = \frac{2(\beta_a\kappa_c - \beta_c\kappa_a)}{\kappa_v} \left[\left(\frac{\partial\omega}{\partial \ln a}\right)_{c,T} - \left(\frac{\partial\omega}{\partial \ln c}\right)_{a,T} \right] \quad (2)$$

where $\kappa_a = s_{11} + s_{12} + s_{13}$, $\kappa_c = s_{33} + 2s_{13}$ (for tetragonal symmetry²⁵), β_a , β_c are the linear compressibilities and thermal expansion coefficients along the a and c axes, respectively, κ_v is the volume compressibility, and s_{ij} is the film compliances. The studies on the $\text{La}_{0.83}\text{Sr}_{0.17}\text{MnO}_3$ compound have shown that it is nearly isotropic in terms of the thermal expansion.²² It is quite probable that the same is true for the compound under investigation, which has the same structure.

As seen from Eq. (1), in the isotropic approximation and in the absence of the explicit (pure anharmonic) term, the temperature and hydrostatic pressure dependences of the two bands at $\sim 268 \text{ cm}^{-1}$ and $\sim 476 \text{ cm}^{-1}$ should be proportional, independent of the exact values of the thermal expansion coefficient and the bulk compressibility. From the temperature dependence (Fig. 5), we can estimate that $d\omega/dT$ has very close values for the two bands at $\sim 268 \text{ cm}^{-1}$ ($0.060 \text{ cm}^{-1}/\text{K}$) and $\sim 476 \text{ cm}^{-1}$ ($0.065 \text{ cm}^{-1}/\text{K}$). On the other hand, from the hydrostatic pressure dependence (measured at room temperature), we induce that $d\omega/dP = 2.1 \text{ cm}^{-1}/\text{GPa}$ and $5.9 \text{ cm}^{-1}/\text{GPa}$ for the two modes, respectively, which clearly are not proportional to the above $d\omega/dT$ values, as expected in the case of isotropic and harmonic behavior of phonons. If, for a rough estimate, we use the value of thermal expansion coefficient of $\text{La}_{0.83}\text{Sr}_{0.17}\text{MnO}_3$,^{21,22} $\text{Pr}_{0.75}\text{Sr}_{0.25}\text{MnO}_3$,²³ or $\text{La}_{0.67}\text{Ca}_{0.33}\text{MnO}_3$,²⁴ we find from Eq. (1) that the softening of the band at $\sim 476 \text{ cm}^{-1}$ with temperature is mainly due to the thermal expansion of the compound. On the other hand, it is clear that for the phonon at $\sim 268 \text{ cm}^{-1}$ the pure anharmonic explicit term is important and/or the isotropic approximation may not be valid. Since the band at $\sim 476 \text{ cm}^{-1}$ involves internal vibrations of the octahedra,^{9,26} it is expected to be more rigid to deformations, as our analysis indicates. Based on the correspondence with a similar mode of $\text{La}_{1-x}\text{Ca}_x\text{MnO}_3$ (Refs. 9,20,26) and its anharmonicity, we believe that the phonon at $\sim 268 \text{ cm}^{-1}$ must involve rotations along the b axis of the octahedra of A_g symmetry, as in the case of LaMnO_3 .⁹ Therefore, this phonon at $\sim 268 \text{ cm}^{-1}$ and the corresponding rotations of the octahedra should be anharmonic, and are affected by the distortions of the MnO_6 octahedra.²⁰ These results agree with the strong softening that has been found for the A_g phonon by Podobedov *et al.*²⁷ and Abrashev *et al.*²⁸ attributed to rotational distortions.²⁸ A similar anharmonic behavior is observed for the mode at $\sim 300 \text{ cm}^{-1}$, which is due to titling vibrations of the octahedra (out of phase x -axis rotations⁹). This phonon is energy independent of temperature in the range $77\text{--}300 \text{ K}$, but it strongly shifts with hydrostatic pressure ($\sim \text{cm}^{-1}/\text{GPa}$, Fig. 8).

V. CONCLUSIONS

We have studied the effect on the Raman spectra from two $\text{Pr}_{0.5}\text{Ca}_{0.5}\text{MnO}_3$ films developed on SrTiO_3 and LaAlO_3 substrates, which develop tensile and compression strains on the

film. Spectral modifications are observed at a temperature, which coincides with the transition temperature for the formation CO. An increase in intensity of two high-energy bands at $\sim 476\text{ cm}^{-1}$ and $\sim 605\text{ cm}^{-1}$ has been observed with three excitation wavelengths at T_{CO} . Moreover, the two modes at 460 cm^{-1} and 476 cm^{-1} appear to have a different scattering selection rules in the films, induced from the different orientation of the substrates and their B_{2g} and $B_{1g,3g}$ symmetries. The transition temperature was found to be the same in the two substrates but a hysteresis effect has been observed. The high-energy modes are related with the Jahn-Teller (JT) distortions and we attribute the intensity changes with temperature to the different way the localization of carriers affects the JT modes. An external mode at $\sim 268\text{ cm}^{-1}$, which involves relative rotations of the octahedra, shows a

strong softening with temperature. Based on the temperature and hydrostatic pressure dependences of the external and internal modes at $\sim 268\text{ cm}^{-1}$, 300 cm^{-1} , and $\sim 476\text{ cm}^{-1}$, the amount of pure anharmonicity is estimated to be strong only for the external vibrational phonons. The strains induced by the two different substrates do not seem to affect the Raman spectra, probably due to their relaxation towards the surface of the films used in our studies.

ACKNOWLEDGMENTS

We would like to thank Dr. G. Varelogiannis for useful discussions and comments. One of the authors (E.L.P.) acknowledges financial support from the GSRT Grant No. 01EP13.

-
- ¹A.P. Ramirez, *J. Phys.: Condens. Matter* **9**, 8171 (1997).
²D.E. Cox, P.G. Radaelli, M. Marezio, and S.-N. Cheong, *Phys. Rev. B* **57**, 3305 (1998).
³V. Dediu, C. Ferdeghini, F.C. Matocotta, P. Nozar, and G. Ruani, *Phys. Rev. Lett.* **84**, 4489 (2000).
⁴Rajeev Gupta, G. Venketeswara Pai, A.K. Sood, T.V. Ramakrishnan, and C.N.R. Rao, cond-mat/0108476 (unpublished).
⁵Y. Tomioka, A. Asamitsu, H. Kuwahara, Y. Moritomo, and Y. Tokura, *Phys. Rev. B* **53**, R1689 (1996).
⁶Y. Tokura and Y. Tomioka, *J. Magn. Magn. Mater.* **200**, 1 (1999) and references therein.
⁷W. Prellier, Ph. Lecoeur, and B. Mercey, *J. Phys.: Condens. Matter* **13**, R915 (2001).
⁸P.G. Radaelli, G. Iannone, M. Marezio, H.Y. Hwang, S-W. Cheong, J.D. Jorgensen, and D.N. Argyriou, *Phys. Rev. B* **56**, 8265 (1997).
⁹M.N. Iliev, M.N. Abrashev, H.-G. Lee, V. N. Popov, Y.Y. Sun, C. Thomsen, R.L. Meng, and C.W. Chu, *Phys. Rev. B* **57**, 2872 (1998).
¹⁰L. Martin-Carron, A. de Andres, M.J. Martinez-Lope, M.T. Casais, and J.A. Alonso, *J. Alloys Compd.* **323–324**, 494 (2001).
¹¹W. Prellier, A.M. Haghiri-Gosnet, B. Mercey, Ph. Lecoeur, M. Hervieu, Ch. Simon, and B. Raveau, *Appl. Phys. Lett.* **77**, 1023 (2000).
¹²A.M. Haghiri-Gosnet, M. Hervieu, Ch. Simon, B. Mercey, and B. Raveau, *J. Appl. Phys.* **88**, 3545 (2000).
¹³Z. Jirak, S. Krupicka, Z. Simsa, M. Doulka, and S. Vratislma, *J. Magn. Magn. Mater.* **53**, 153 (1985).
¹⁴W. Prellier, Ch. Simon, A.M. Haghiri-Gosnet, B. Mercey, and B. Raveau, *Phys. Rev. B* **62**, R16 337 (2000).
¹⁵M. Lax, *Appl. Phys. Lett.* **33**, 786 (1978).
¹⁶E. Liarokapis and Y.S. Raptis, *J. Appl. Phys.* **57**, 5123 (1985).
¹⁷M.N. Abrashev, J. Backstrom, L. Borjesson, M. Pissas, N. Kolev, and M.N. Iliev, *Phys. Rev. B* **64**, 144429 (2001).
¹⁸P.B. Allen and V. Perebeinos, *Phys. Rev. Lett.* **83**, 4828 (1999).
¹⁹D.N. Argyriou, H.N. Bordallo, B.J. Campbell, A.K. Cheetham, D.E. Cox, J.S. Gardner, K. Hanif, A. dos Santos, and G.F. Strouse, *Phys. Rev. B* **61**, 15 269 (2000).
²⁰E. Liarokapis, Th. Leventouri, D. Lampakis, D. Palles, J.J. Neumeier, and D.H. Goodwin, *Phys. Rev. B* **60**, 12 758 (1999).
²¹T.W. Darling, A. Migliori, E.G. Moshopoulou, Stuart A. Trugman, J.J. Neumeier, J.L. Sarrao, A.R. Bishop, and J.D. Thompson, *Phys. Rev. B* **57**, 5093 (1998).
²²J.J. Neumeier, K. Andres, and K.J. McClellan, *Phys. Rev. B* **59**, 1701 (1999).
²³S.T. Aruna, M. Muthuraman, and K.C. Patil, *Solid State Ionics* **120**, 275 (1999).
²⁴G. Zhao, M.B. Hunt, and H. Keller, *Phys. Rev. Lett.* **78**, 955 (1997).
²⁵P.S. Peercy, *Phys. Rev. B* **8**, 6018 (1973).
²⁶M.V. Abrashev, J. Backstrom, L. Borjesson, V.N. Popov, R.A. Chakalov, N. Kolev, R.-L. Meng, and M.N. Iliev, *Phys. Rev. B* **65**, 184301 (2002).
²⁷V.B. Podobedov, A. Weber, D.B. Romero, J.P. Rice, and H.D. Drew, *Solid State Commun.* **105**, 589 (1998).
²⁸M.V. Abrashev, A.P. Litvinchuk, M.N. Iliev, R.L. Meng, V.N. Popov, V.G. Ivanov, R.A. Chakalov, and C. Thomsen, *Phys. Rev. B* **59**, 4146 (1999).